

YOUN JI HEO^{1,2}, EUI SEON LEE¹, JEONG HYUN KIM¹, YOUNG-IN LEE^{1,2},
YOUNG-KEUN JEONG³, SUNG-TAG OH^{1,2*}

SYNTHESIS AND CHARACTERIZATION OF W COMPOSITE POWDER WITH La₂O₃-Y₂O₃ NANO-DISPERSOIDS BY ULTRASONIC SPRAY PYROLYSIS

An optimum route to synthesis the W-based composite powders with homogeneous dispersion of oxide nanoparticles was investigated. The La₂O₃ dispersed W powder was synthesized by ultrasonic spray pyrolysis using ammonium metatungstate hydrate and lanthanum nitrate. The dispersion of Y₂O₃ nanoparticles in W-La₂O₃ powder was carried out by a polymer addition solution method using yttrium nitrate. XPS and TEM analyses for the composite powder showed that the nano-sized La₂O₃ and Y₂O₃ particles were well distributed in W powder. This study suggests that the combination processing of ultrasonic spray pyrolysis and polymeric additive solution is a promising way to synthesis W-based composite powders.

Keywords: W composite powder; La₂O₃-Y₂O₃ dispersion; Ultrasonic spray pyrolysis; Polymeric additive solution method

1. Introduction

Tungsten (W) is suitable for various high temperature applications due to its unique properties such as high density, high melting point, low thermal coefficient, and high temperature strength [1-3]. However, W has disadvantages such as poor ductility, high ductile-brittle transition temperature (DBTT), low fracture toughness and low recrystallization brittleness. To solve these problems, W-based composites with dispersion of nano-sized oxide particles have been developed by mechanical alloying and wet chemical process [4-5], because the oxide nanoparticles inhibit recrystallization and reduce the DBTT to improve the brittleness. However, the previously developed method has difficulty in uniformly dispersing nano-sized particles.

Motivated by an interest in homogeneous dispersion control of oxide nanoparticles, we investigated the feasibility of the fabrication of W composite with Y₂O₃ and La₂O₃ nanoparticles by wet chemical methods [6,7]. This earlier study indicated that the microstructure having homogeneous distribution of oxide nanoparticles could be achieved by the processing. In the present approach, the W-La₂O₃-Y₂O₃ composite powders are synthesized, and their microstructural characteristics are analyzed. W powder dispersed with La₂O₃ particles was prepared by ultrasonic spray

pyrolysis (USP). Subsequently, Y₂O₃ particles were coated on their surface by polymer addition solution method. An optimum synthesis condition is suggested based on the observed microstructural characteristics of composite powders.

2. Experimental

W-1 wt% La₂O₃ powder was prepared by USP using the precursors of ammonium metatungstate hydrate [(NH₄)₆H₂W₁₂O₄₀·xH₂O, Sigma Aldrich] and lanthanum (III) nitrate 6-hydrate [La(NO₃)₃·6H₂O, Sigma Aldrich]. Precursors with concentration of 100 mM was dissolved in distilled water and nebulized into microdroplets by ultrasonic energy with a frequency of 1.7 MHz. Then, the aerosol droplets were sent into furnace heated to the first zone at 200°C and the second zone at 700°C using N₂ carrier gas at a flow rate of 2 L/min. The WO₃-La₂O₃ powder was collected by the incorporation of a filter paper in the carrier gas stream. To obtain W-1 wt% La₂O₃ powder, hydrogen reduction of collected powder at 800°C for 1 h was conducted. To fabricate W-1 wt% La₂O₃-1 wt% Y₂O₃ powder, the polymer addition solution method using yttrium (III) nitrate 6-hydrate [Y(NO₃)₃·6H₂O, Sigma Aldrich] was applied. The detailed procedure is described elsewhere [6].

¹ SEOUL NATIONAL UNIVERSITY OF SCIENCE AND TECHNOLOGY, DEPARTMENT OF MATERIALS SCIENCE AND ENGINEERING, SEOUL 01811, REPUBLIC OF KOREA

² SEOUL NATIONAL UNIVERSITY OF SCIENCE AND TECHNOLOGY THE INSTITUTE OF POWDER TECHNOLOGY, SEOUL 01811, REPUBLIC OF KOREA

³ PUSAN NATIONAL UNIVERSITY, GRADUATE SCHOOL OF CONVERGENCE SCIENCE, BUSAN 46241, REPUBLIC OF KOREA

* Corresponding author: stoh@seoultech.ac.kr



The morphology of the powders was observed by field emission scanning electron microscopy (FE-SEM, JSM-6700F, JEOL Ltd.). Phase identification of the synthesized powders was determined by X-ray diffraction analysis (XRD, Dmax2500, Rigaku). Also, element composition and chemical bonding of the powder were determined by high-performance X-ray photoelectron spectroscopy (HR-XPS, K-Alpha+, Thermo Scientific). High resolution transmission electron microscope (HR-TEM, NEO ARM, JEOL Ltd.) and energy dispersive X-ray spectrometer (EDS) were used for the analysis of crystallographic structure and element composition.

3. Results and discussion

Typical morphologies of powders at different stages of processing are observed by SEM. As shown in Fig. 1(a), the synthesized W powder by USP and hydrogen reduction exhibited a spherical shape with porous structure due to the reduction of W oxides. Fig. 1(b) and (c) show the composite powders of W-1 wt% La_2O_3 by USP and W-1 wt% La_2O_3 -1 wt% Y_2O_3 by polymeric additive solution route, respectively. The composite powders showed a spherical shape but exhibited a finer size than the pure tungsten powder synthesized with USP. On the other hand, in the microstructure of the composite powders, some cube-shaped particles are observed as indicated by arrows. In general, W powder has a tendency being cube shape as the

degree of oxidation increases [8,9]. Thus, it is interpreted that the formation of these particles is due to the formation of some oxides during the synthesis process of the composite powder. This result suggests that hydrogen reduction for 1 h was not sufficient to fabricate the composite powder with pure W.

XRD result for the composite powder of W-1 wt% La_2O_3 -1 wt% Y_2O_3 is shown in Fig. 2. The diffraction line corresponding to α -W can be observed. Meanwhile, the existence of La_2O_3 and Y_2O_3 phases are not observed because of the limit of XRD resolution. For a more detailed phase analysis for La_2O_3 and Y_2O_3 , the chemical state of the composite powder is investigated by XPS.

Fig. 3 shows high-resolution narrow-scan XPS spectra of W4f, La3d, Y3d and O1s of W-1 wt% La_2O_3 -1 wt% Y_2O_3 powder. As clearly seen in Fig. 3(a), the chemical binding energy (31.3 and 33.4 eV) of metal tungsten is mainly observed, but peaks at higher binding energies are also observed. These peaks at binding energies of 31.9, 35.2 and 35.8 eV are identified as W^{4+} , W^{5+} and W^{6+} , respectively [10]. Thus, it is indicated that trace amounts of metallic tungsten are bound with oxygen in the composite powder. Fig. 3(b) shows the La3d spectrum, and the peak at binding energy of 834.7 eV are identified as La^{3+} which means La_2O_3 phase in comparison with O1s spectra in Fig. 3(d) [11]. The peaks at 159.7 and 157.7 eV in Y3d spectrum were observed and they correspond to Y_2O_3 phase [12].

In order to further reveal the detailed microstructure and composition of the composite powders, the fast Fourier transform

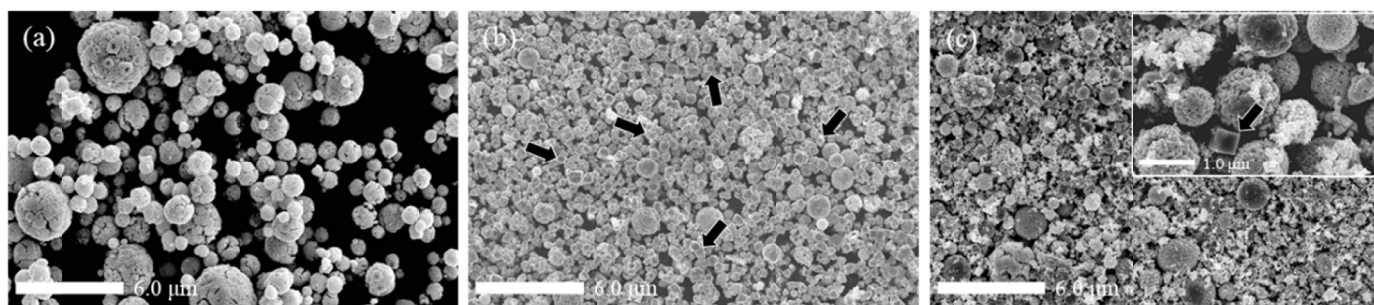


Fig. 1. SEM micrographs of powders at different stages of processing: (a) W powder by USP and hydrogen reduction, (b) W-1 wt% La_2O_3 powder by USP and hydrogen reduction, (c) W-1 wt% La_2O_3 -1 wt% Y_2O_3 powder by calcination and hydrogen reduction

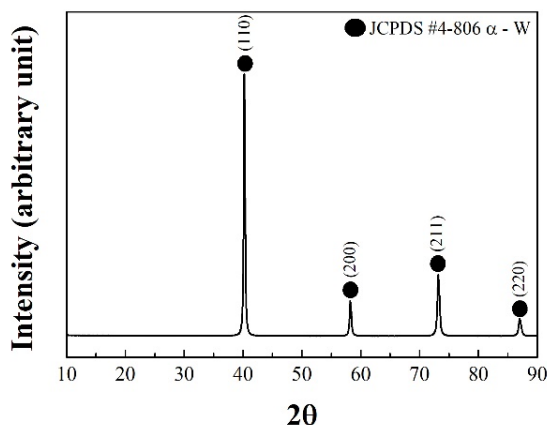


Fig. 2. XRD profile of W-1 wt% La_2O_3 -1 wt% Y_2O_3 powder prepared by polymeric additive solution route and hydrogen reduction

(FFT) pattern of the HR-TEM are analyzed. As shown in Fig. 4, the selected area electron diffraction (SAED) of the powder reveals the existence of W, Y_2O_3 , and La_2O_3 . Also, in HR-TEM image and fast Fourier transform (FFT) patterns, (002), (101) and (110) planes of hexagonal La_2O_3 as well as ($2\bar{2}0$), ($\bar{4}40$) and ($2\bar{6}2$) planes of cubic Y_2O_3 were detected [13,14].

TEM observation and EDX mapping were performed as shown in Fig. 4(f). It clearly reveals that La and Y elements are distributed homogeneously in composite powder. From these observations, it is suggested that ultrasonic spray pyrolysis and polymer addition solution method are useful for producing W powders with homogeneously dispersed La_2O_3 and Y_2O_3 nanoparticles.

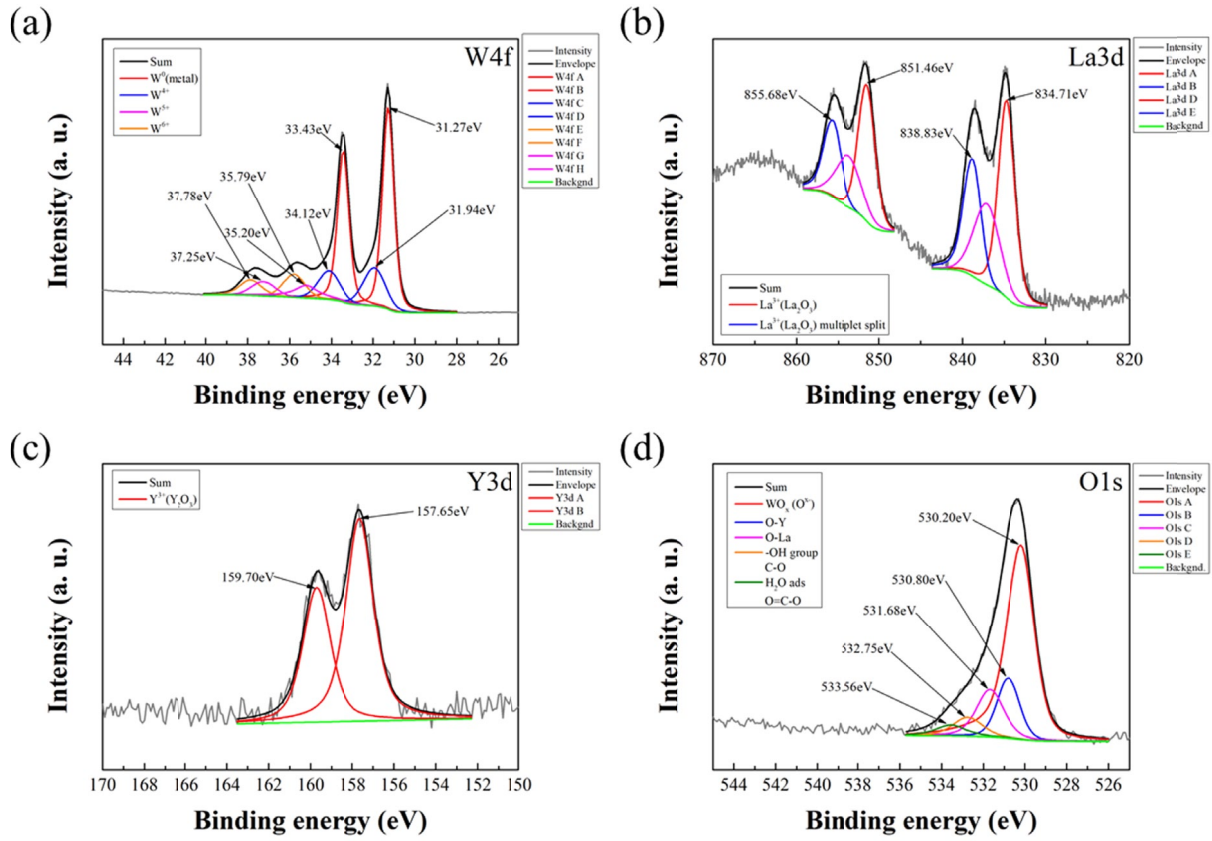


Fig. 3. XPS profiles of W-1 wt% La₂O₃-1 wt% Y₂O₃ powder for (a) W4f, (b) La3d, (c) Y3d and (d) O1s

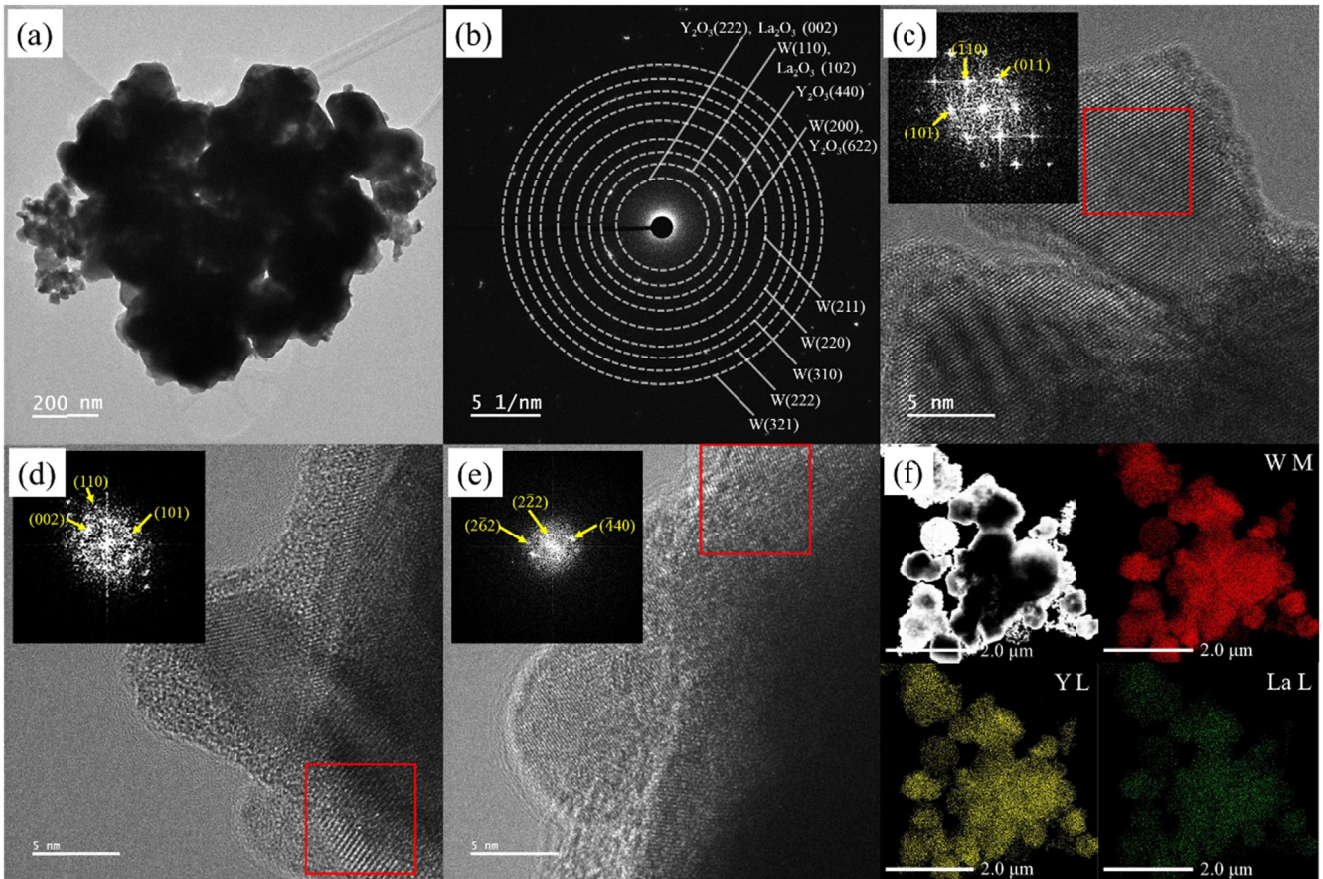


Fig. 4. HR-TEM analysis of composite powder; (a) TEM image, (b) SAED pattern, (c) FFT pattern of W, (d) FFT pattern of La₂O₃, (e) FFT pattern of Y₂O₃ and (f) TEM-EDX image

4. Conclusions

An optimum route to synthesize the W composite powder with homogeneously dispersed La_2O_3 and Y_2O_3 nanoparticles was investigated. The W- La_2O_3 powder was prepared by the ultrasonic spray pyrolysis and hydrogen reduction. The composite powder with homogeneously coated Y_2O_3 particles on W- La_2O_3 was synthesized by the polymeric additive solution route. Although some tungsten oxide was present in the synthesized composite powder, microstructure analysis using TEM and XPS revealed that W powder with a uniform distribution of La_2O_3 and Y_2O_3 nanoparticles can be fabricated. This study suggests that the ultrasonic spray pyrolysis combined with wet chemical method is one of the promising ways to fabricate W-based composite powders with homogeneous dispersion of oxide nanoparticles.

Acknowledgments

This work was supported by the National Research Foundation of Korea (NRF) grant funded by the Korea government (MSIT) (2019R1A2B5B01070587).

REFERENCES

- [1] H. Wang, Z.Z. Fang, K.S. Hwang, H. Zhang, D. Siddle, *Int. J. Refrac. Met. H.* **28**, 312-316 (2010).
- [2] Z.S. Levin, K.T. Hartwig, *Mater. Sci. Eng.* **707**, 602-611 (2017).
- [3] W.J. Choi, J.H. Kim, H. Lee, C.W. Park, Y.-I. Lee, J. Byun, *Int. J. Refrac. Met. H.* **95**, 105450-105458 (2021).
- [4] Z. Dong, N. Liu, Z. Ma, C. Liu, Q. Guo, Y. Liu, *J. Alloy. Compd.* **95**, 2969-2973 (2017).
- [5] S. Park, D.-K. Kim, S. Lee, H.J. Ryu, S.H. Hong, H.J. Ryu, *Metall. Mater. Trans. A.* **32**, 2011-2020 (2001).
- [6] H. Jo, Y.-I. Lee, M.-J. Suk, Y.-K. Jeong, S.-T. Oh, *Arch. Metall. Mater.* **66**, 799-802 (2021).
- [7] E.S. Lee, G. Lee, Y.-I. Lee, Y.-K. Jeong, S.-T. Oh, *Powder Metall.* **64**, 108-114 (2021).
- [8] M. Weil, W.-D. Schubert, "The beautiful colors of Tungsten oxides", *ITIA Newsl.* 1-12 (2013).
- [9] X. Zhang, Z. Gong, J. Huang, B. Yu, *Mater. Res. Express* **7**, 56513-56522 (2020).
- [10] F.Y. Xie, L. Gong, X. Liu, Y.T. Yao, W.H. Zhang, S.H. Chen, H. Meng, J. Chen, *J. Electron. Spectrosc.* **185**, 112-118 (2012).
- [11] E. Baskys, V. Bondarenka, S. Grebinskij, M. Senulis, R. Sereika, *Lith. J. Phys.* **43**, 120-124 (2014).
- [12] D. Barreca, G.A. Battiston, D. Berto, *Surf. Sci. Spectra* **8**, 234-239 (2001).
- [13] P. Huang, Y. Zhao, J. Zhang, Y. Zhu, Y. Sun, *Nanoscale* **5**, 10844-10848 (2013).
- [14] W. Hu, Q. Ma, Z. Ma, Y. Huang, Z. Wang, Y. Liu, *Tungsten* **1**, 220-228 (2019).